E831-doc-701-v2
July 13, 2004

Search For the SELEX $D_{sJ}(2632)$ in the DK Final State at FOCUS

Rob Kutschke
For the FOCUS Collaboration

Abstract

This note reports preliminary results, using the FOCUS spectrometer at Fermilab, of a search for a new state, the $D_{sJ}(2632)$, recently reported by SELEX. The state was searched for in the decay modes D^0K^+ and $D^+K^0_S$. No signal is seen in either decay mode. We report our result as an upper limit on the ratio, R, of the cross-section times branching ratio for the $D_{sJ}(2632)$ divided by that for the well established $D^*_{s2}(2572)$. For a narrow state, with a line-shape dominated by the detector resolution, we find $R < 5.3\%$ at the 90% confidence level For a state with a natural width of 17 MeV, the upper limit reported by SELEX, we find $R < 13\%$, at the 90% confidence level. The errors in this analysis are statistical only. SELEX does not report their measured value of R but we estimate it from from information contained in their paper. For a narrow state the FOCUS and SELEX values of R are consistent at less than the 3% confidence level. For a state with a natural width of 17 MeV, the FOCUS and SELEX values agree at less than the 5% CL.

1 Introduction

This note is motivated by a recent paper[1] by the SELEX collaboration in which they report a new state decaying to $D_s\eta$ and D^0K^+. They refer to this state as the $D_{sJ}(2632)$. The masses reported by SELEX are 2635.9 ± 2.9 MeV in the $D_s\eta$ mode and 2631.5 ± 1.9 MeV in the D^0K^+ mode. The errors are statistical only. The mean of these masses is 2632.8 ± 1.6 MeV. SELEX reports that their signal is consistent with their detector resolution and that the upper limit on the natural width of the state is 17 MeV, at the 90% CL.

This note will report on a search for this state using the decay chains D^0K^+, where $D^0 \to K^-\pi^+$ or $K^-\pi^+\pi^+\pi^-$, and $D^+K^0_S$, where $D^+ \to K^-\pi^+\pi^+$ and $K^0_S \to \pi^+\pi^-$. The cuts used to select candidates are given in Appendix A.

2 Results Without the SELEX State

The data points in Figure 1 show the mass difference distribution for DK candidates which pass the selection criteria described in Appendix A. In each histogram the structure near a mass difference of 0.7 GeV/c^2 is the well established $D_{s2}^*(2572)$ and the narrow structure near a mass difference of 0.52 GeV/c^2 is feed-down from the process $D_{s1}(2536) \rightarrow D^*K$, where the D^* decays to D plus unobserved neutrals. Because of the small Q values in these decays, there is little kinematic broadening in the line-shape of the feed-down. Superimposed on the data points is the result of a fit which is described below.

1. The fits were done in 1 MeV bins. This histogram and the fit results were rebinned after the fit for presentation purposes.

2. The fits were done using the binned maximum likelihood method.

3. Each histogram is described by the following sum of terms:

    (a) D-wave Breit-Wigner, convoluted with a gaussian resolution function, to parameterize the D_{s2}^*. The sigma of each gaussian was fixed to the value determined by a Monte Carlo simulation of the detector response. The values of the resolutions are 4.6 MeV for the D^0K^+ and 3.6 MeV for $D^+K_S^0$.

    (b) E687 background function: $A(x - x_t)^B \exp(-C(x - x_t))$, where x is the mass difference, x_t is the threshold in mass difference and where A, B and C are parameters to be determined by the fit.

    (c) A term for the feed-down from the D_{s1}. This term has a fixed shape, determined by an MC simulation of the detector response, and a free yield.

    (d) The decay mode $D_{s2}^* \rightarrow D^*K$ is allowed but the branching fraction is suppressed by the small Q value of the decay. This decay would appear in these histograms as a second, broader feed-down peak. The fit includes a term for this feed-down, again with a fixed shape, determined by a Monte Carlo simulation of the detector response, and a free yield.

4. Simultaneous fit to both histograms. The mass and with of the D_{s2}^* are the same for both histograms. There were a total of 14 free parameters in the fit:

    (a) 2: Mass and width of D_{s2}^*, common to both plots.

    (b) 2: The yield of the D_{s2}^* in each of the two decay modes.

    (c) 10: 5 background and feed-down parameters for each of the histograms:

Model	Mass (MeV/c^2)	Γ (MeV/c^2)	R (%) (90% CL Upper Limit, in %) D^0K^+		$D^+K^0_S$	
1	2635.9	0	2.2 ± 2.2	(< 5.3)	-2.8 ± 4.3	(< 5.4)
2	2631.5	0	3.0 ± 2.2	(< 5.9)	2.3 ± 4.2	(< 8.4)
3	2635.9	17	11.2 ± 4.6	$(< 17.)$	-9.2 ± 9.6	$(< 11.)$
4	2631.5	17	10.6 ± 4.7	$(< 16.)$	-5.3 ± 9.7	$(< 13.)$

Table 1: The first three columns describe four different parameterizations of the SELEX state that are used in the fits. For models with $\Gamma = 0$ the line-shape was parameterized as a gaussian with σ given by the resolution of the FOCUS detector. For models with $\Gamma = 17$ MeV the line-shape was parameterized as a Breit-Wigner with $\Gamma = 17$ MeV, convoluted with a gaussian resolution function. The fourth and sixth columns give the measured value of R for each of the two decay modes. And the fifth and seventh columns give the 90% CL upper limit on R. All errors are statistical only.

i. 3: Parameters of the E687 background shape.
ii. 2: Yields of the two feed-downs.

5. After completion of the fit, a χ^2 was computed to compare the fit results with the data. A confidence level was computed from this χ^2.

The confidence level of the fit and the fitted values of the interesting parameters are shown on the figure. The errors are statistical only and a systematics study is underway. The yield of the feed-down from the D^*_{s2} is not stable with cut variations and no signal is claimed.

A mini-MC study was done to ensure that the fit procedure produces unbiased central values, correct errors and a confidence level distribution which is flat. In this study, 100 trial histograms were drawn using the fit result as the source distribution. Each of these trial histograms was fitted using the same procedure as was the data. The results show that the fit procedure works correctly. In particular it shows that the confidence level has a flat distribution. So the observed confidence level of 0.65 indicates a good overall fit.

3 Results with the SELEX State Included

In Figures 2 through 5 a term has been added to the fit to allow for the presence of the SELEX state. In order to cover the parameter space allowed by the SELEX paper, four different parameterizations were tried for the line-shape of the SELEX state. These line-shapes are described in Table 1. It was presumed, without checking, that the resolution on the mass difference is the same at the mass of the SELEX state as it was at the mass of the D^*_{s2}.

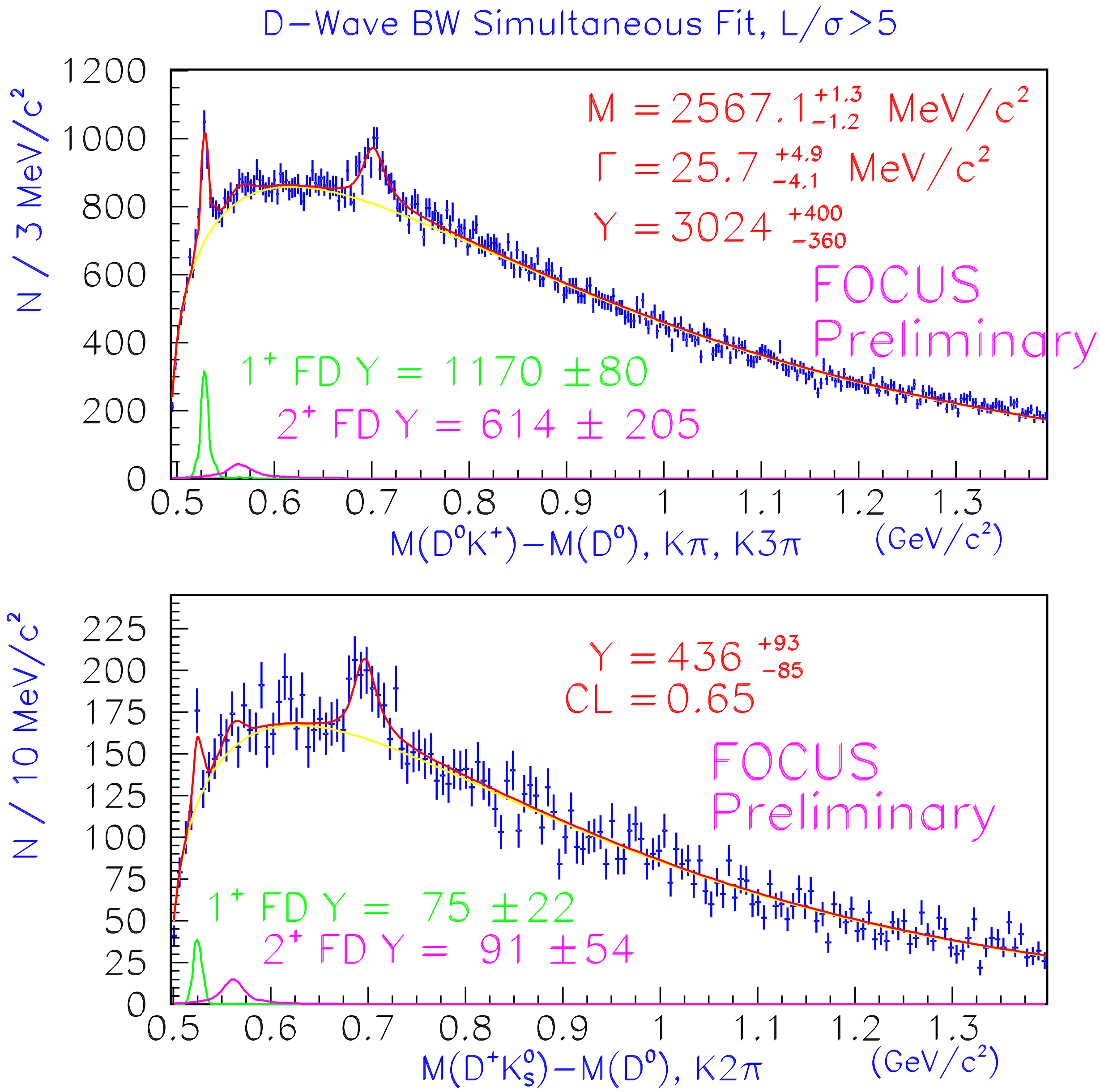

Figure 1: Simultaneous fit to the D^0K^+ and $D^+K^0_S$ mass difference distributions, without allowing for the SELEX state. The superimposed curves show the results of a fit described in the text. The red curve shows the full result of the fit. The yellow curve shows the contribution from the E687 background function. The green and magenta curves show the contributions from the two feed-down terms. The numerical values of the results returned by the fit are shown with their statistical errors.

Figure 2 shows the same data as Figure 1, but zoomed into the region of interest and rebinned. In this case the fit model has the terms described earlier plus model 1 of the SELEX line-shape. This adds two new free parameters to the fit, one for the yield of the SELEX state in $D^0 K^+$ and one for its yield in $D^+ K^0_S$. The fit was done over the full mass range shown in Figure 1, but only the region of interest is shown. The fit was done in 1 MeV bins and rebinned for presentation purposes. The superimposed red curve shows the full fit function and the superimposed blue curve shows the E687 background function. The red arrow shows the mass difference corresponding to a mass of 2635.9 MeV, the value reported in the SELEX $D_s\eta$ analysis. The signal yields and the confidence level of the fit are noted on the figure. No signal is observed at the mass of the SELEX state.

To make a quantitative statement about the production rate of the SELEX state, its yield will be normalized to that of the well established D^*_{s2}. We define a ratio of cross-section times branching ratio,

$$R = \frac{\sigma(\gamma N \to D_{sJ}(2632)X)\mathcal{B}(D_{sJ}(2632) \to DK)}{\sigma(\gamma N \to D^*_{s2}X)\mathcal{B}(D^*_{s2} \to DK)} = \frac{\text{Yield}(D_{sJ}(2632))}{\text{Yield}(D^*_{s2})} \quad (1)$$

A Monte Carlo simulation of the detector response shows that the efficiency of the FOCUS detector changes by less than 1% over the mass range of 2570 to 2630 MeV/c^2. Therefore the above formula does not contain a correction for the relative reconstruction efficiency of the two states. Using the yields reported by the fit gives the ratio $R = 2.2 \pm 2.2\%$. The values of R for the four models of the SELEX line-shape are reported in Table 1.

To determine the 90% CL upper limit on R, the following procedure was used. Given the measured value of R, R_0, and the error on R, σ_R, solve for the 90% CL limit, R_{90},

$$0.90 = \frac{\int_0^{R_{90}} N(R_0, \sigma_R)dy}{\int_0^{\infty} N(R_0, \sigma_R)dy} \quad (2)$$

where $N(R_0, \sigma_R)$ is a normal distribution with a mean of R_0 and a width of σ_R. The upper limit obtained by this procedure is given in Table 1.

Figures 3 through 5 are the same as Figure 2 but using the other three models for the line-shape of the SELEX state. The limits on R obtained from these fits are also summarized in Table 1.

Ignoring phase space effects that are presumably small, the $D^0 K^+$ and $D^+ K^0_S$ channels give independent measurements of the same R. So the final FOCUS measurement of R is just the weighted mean of the measurements for the two channels. This mean is reported in Table 2. The 90% CL upper limit on the combined R was computed as described above and is also reported in Table 2.

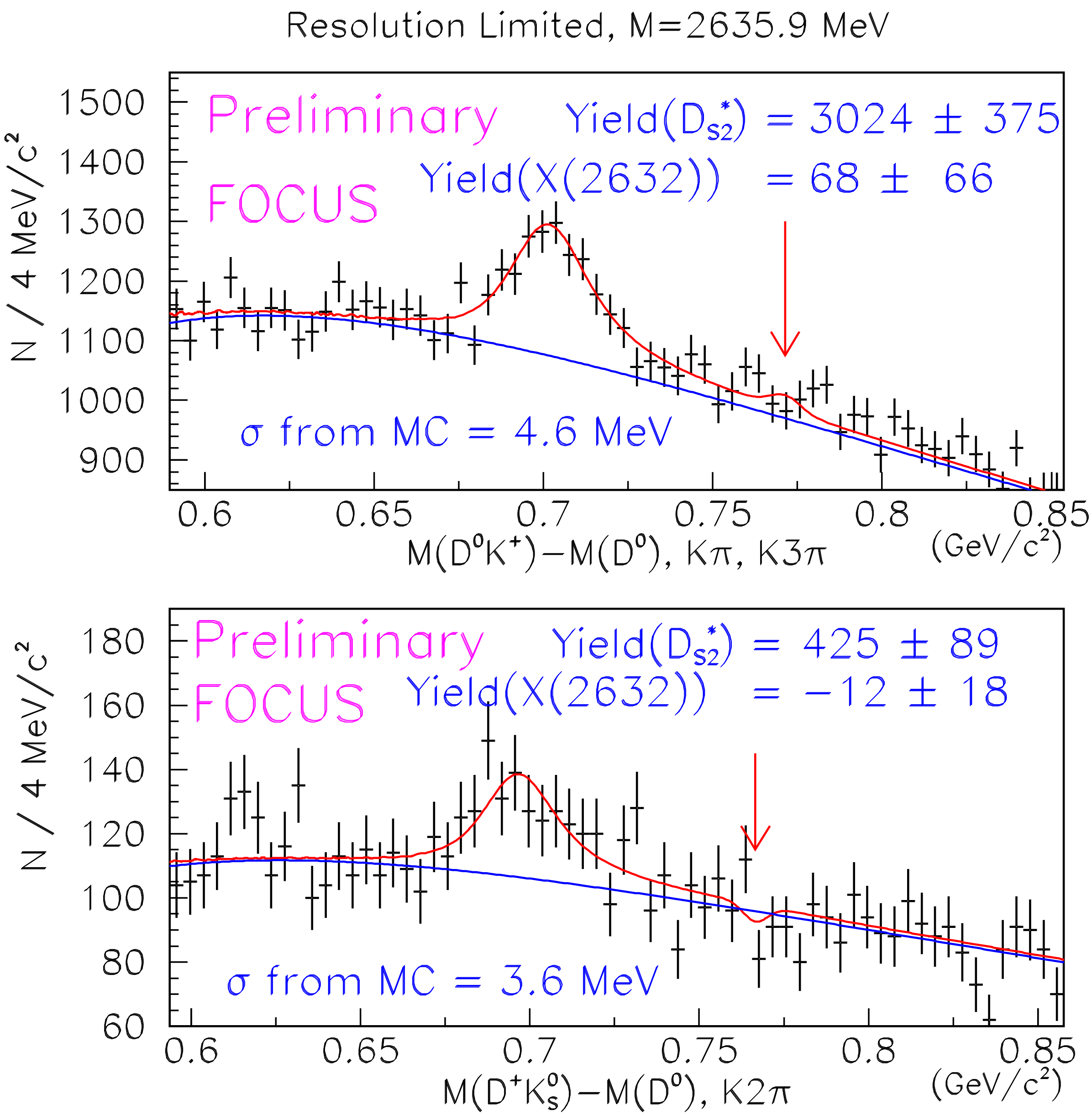

Figure 2: Same data as shown in Figure 1, zoomed into the region of the SELEX state and rebinned. The fit model has been expanded to include the model 1 parameterization of the line-shape of the SELEX state. The arrow marks the expected position of the SELEX state.

Model	R (%)	R_{90} (%)	CL vs SELEX
1	1.2 ± 2.0	4.1	0.025
2	2.8 ± 1.9	5.3	0.029
3	7.4 ± 4.1	12.7	0.045
4	7.6 ± 4.2	13.1	0.046

Table 2: The second and third columns give the values of R and R_{90} using the weighted mean of the D^0K^+ and $D^+K_S^0$ channels. The errors are statistical only. The last column gives the confidence level that this value of R agrees with our estimate of the SELEX value of R. Our estimate of the SELEX value, 0.64 ± 0.28, is described in the text.

4 Comparison with SELEX Results

The SELEX paper does not report the ratio R but it can be estimated from their Figure 3. By counting bin contents in the dark shaded regions, I estimate yields of 21.7 ± 6.2 for the D_{s2}^* and 14 ± 4.6 for their new state. In this estimate, the quoted uncertainty in the yields is statistical only and is computed as the square root of the sum of the bin contents in the shaded regions; this is equivalent to making the optimistic assumption that the background shape and level have been determined without error. These estimates give $R = 0.64 \pm 0.28$, where the error is statistical only.

The last column of Table 2 gives the confidence level that SELEX estimate of R and the various FOCUS estimates are consistent with each other. The agreement is poor but some sources of error have been neglected in this analysis.

5 Conclusions

The SELEX signal is not seen in the FOCUS DK data. The 90% CL upper limit on the cross-section times branching ratio, normalized to that of the D_{s2}^* is 5.3% for a narrow state and about 13.% for a state with a natural width of 17 MeV. This is much smaller than value of R which we estimate from the SELEX data and the two experiments agree at less than the 5% confidence level.

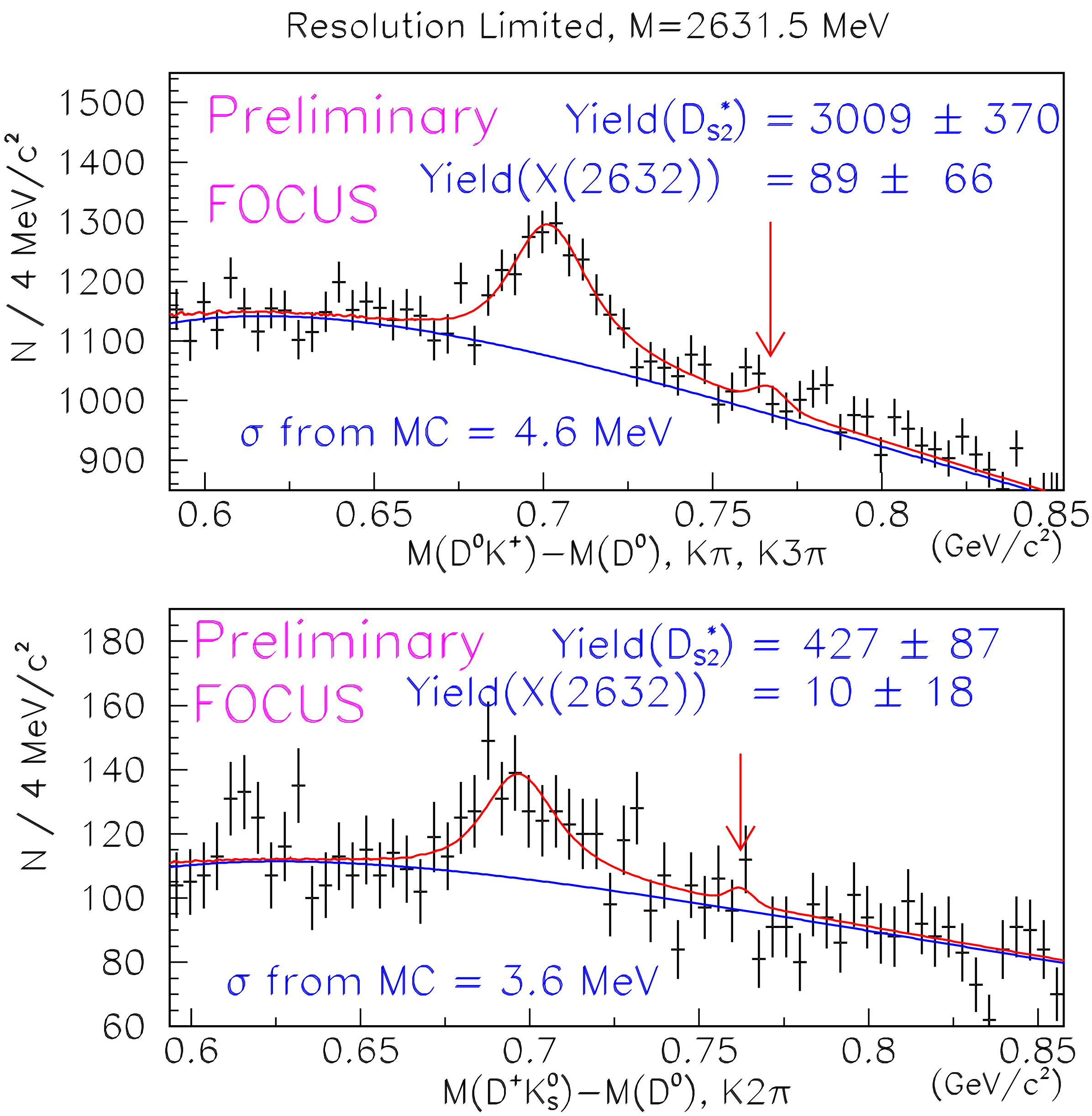

Figure 3: The same as Figure 2 except that line-shape of the SELEX state uses model 2. The arrow marks the expected position of the SELEX state.

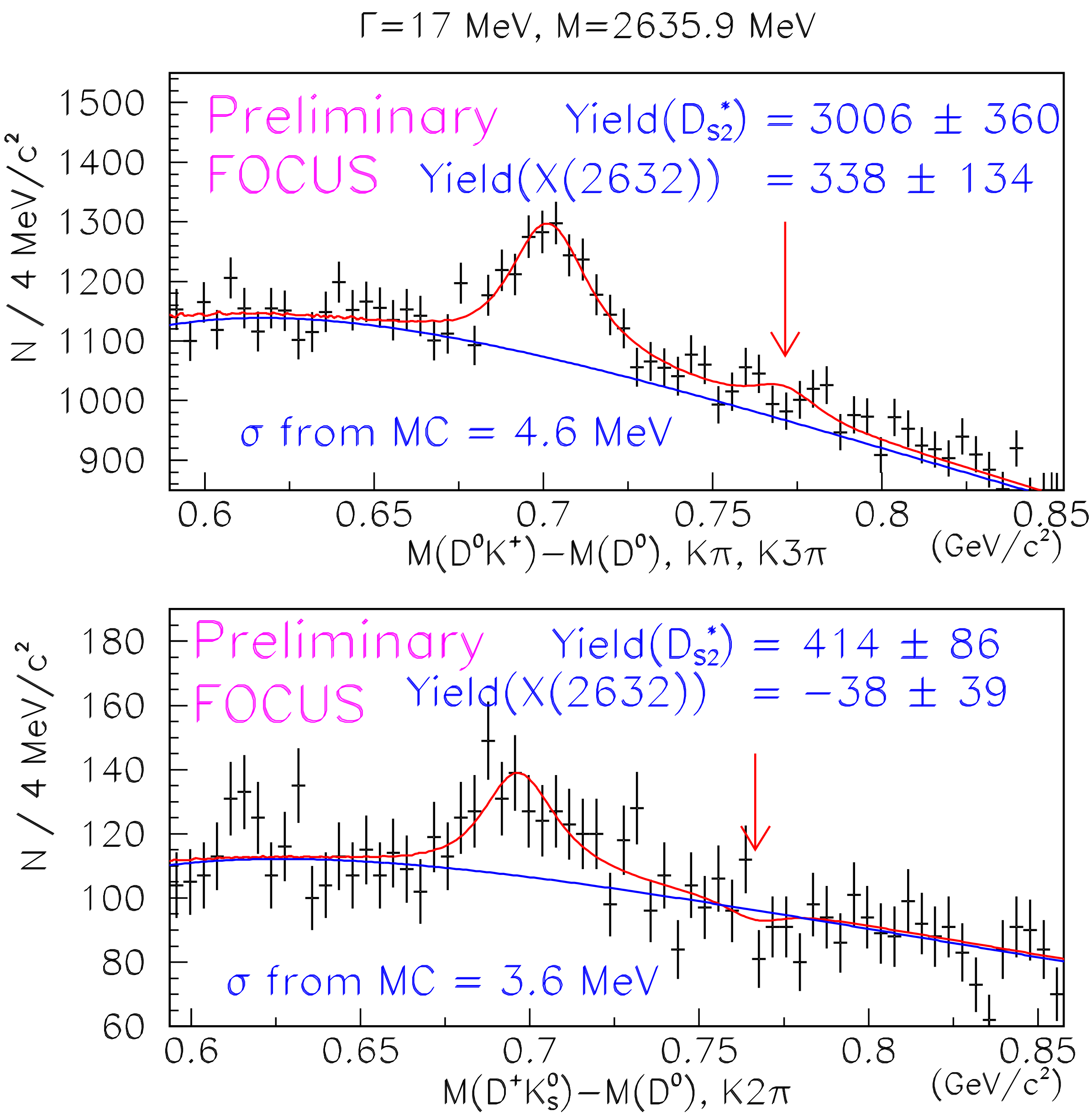

Figure 4: The same as Figure 2 except that the line-shape of the SELEX state uses model 3. The arrow marks the expected position of the SELEX state.

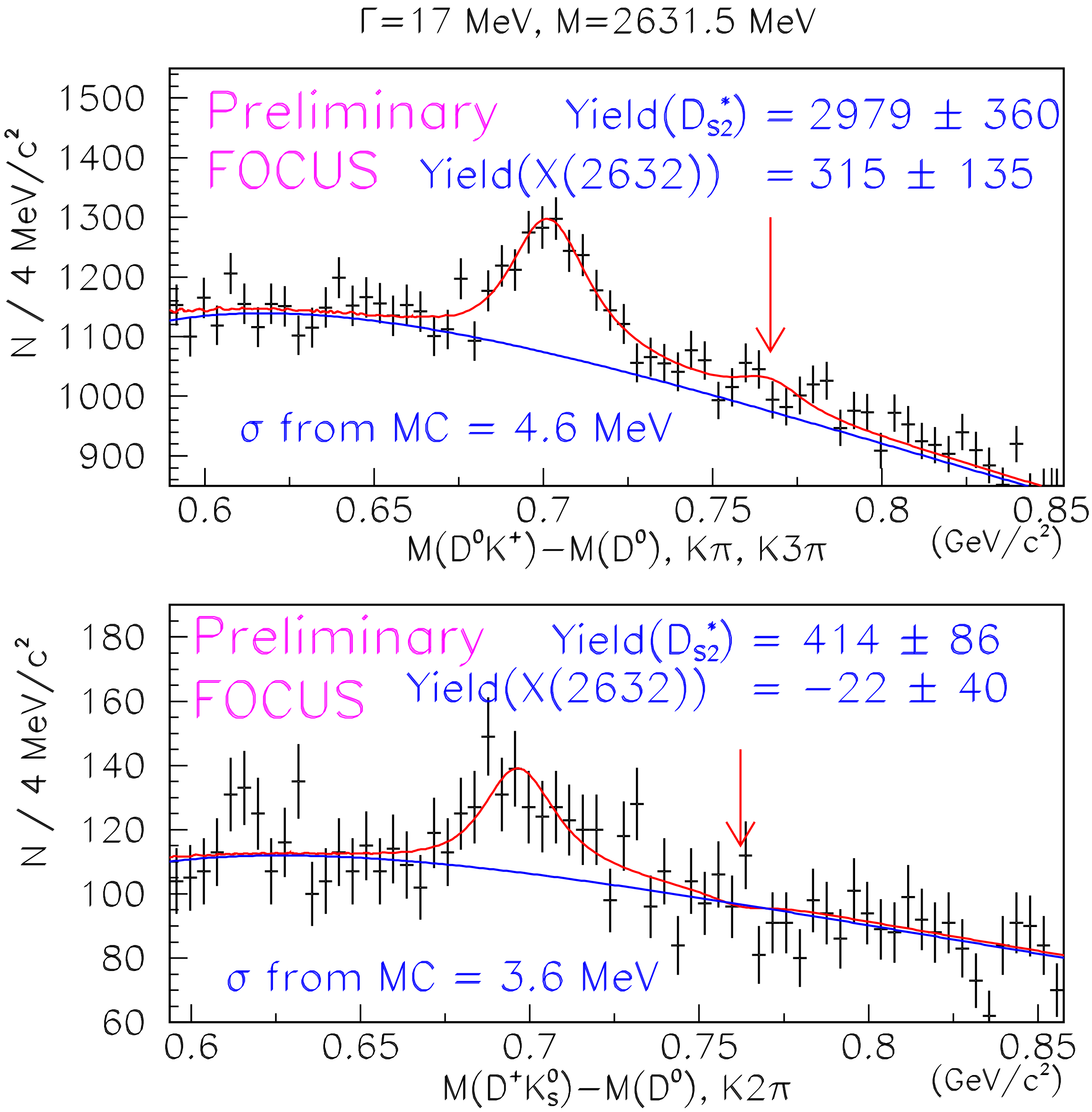

Figure 5: The same as Figure 2 except that the line-shape of the SELEX state uses model 3. The arrow marks the expected position of the SELEX state.

A Summary of Cuts

The lists below give the cuts used to select the combinations shown in the above histograms. They are not necessarily the final cuts but they are good enough for the present study and the $D_{sJ}(2632)$ results are not sensitive to cut variations.

Candidates for charmed mesons were found using the standard FOCUS candidate driven vertexing algorithm, which is the same as that used by the E687 collaboration[2]. Unless otherwise stated it is required that the tracks which form the candidate charmed meson pass a vertex fit with a confidence level > 0.01. The charmed meson candidate is then used to seed a search for a primary vertex. Unless otherwise stated, it is required that a primary vertex be found and that it contain the charm candidate plus at least one other track.

Particle Identification was done using the FOCUS muti-cell threshold Cherenkov system[3]. This system produces a χ^2-like variable which measures how well the measured Cherenkov light distribution satisfies a given mass hypotheses. There is only a small contribution from electrons or protons faking either K or π so the particle ID discussed below concentrates on K/π separation.

The FOCUS K^0_S finding methods and its K^0_S classification scheme is described in reference [4].

A.1 Cuts Used to Select D^0K^+ Combinations

1. D^0 decay modes: $K^-\pi^+$ and $K^-\pi^+\pi^+\pi^-$.
2. For D^0 candidates, $L/\sigma_L > 5$.
3. $1.84 \leq M(K^-\pi^+) < 1.89$ MeV/c^2 or $1.845 \leq M(K^-\pi^+\pi^+\pi^-) < 1.885$ MeV/c^2
4. Affirmative K/π separation for both K: K hypothesis is preferred over π by 2 units of χ^2. ($\Delta WOBS > 2$).
5. Loose consistency on all pions: χ^2 for the π hypothesis no more than than 3 units below that for the than K or p hypothesis.
6. Primary vertex must contain the D^0 plus 2 or more other tracks. The bachelor K must be one of these tracks.
7. The bachelor K is constrained to come from the vertex defined by the other tracks in the primary. The CL of this constraint must be > 0.01. This improves the mass difference resolution, particularly at low mass differences.

A.2 Cuts Used to Select $D^+K^0_S$ Combinations

1. Decay modes: $D^+ \to K^-\pi^+\pi^+$ and $K^0_S \to \pi^+\pi^-$.

2. CL of D^+ vertex fit > 0.05.

3. For D^+: $L/\sigma_L > 5$.

4. $1.845 \leq M(K^-\pi^+\pi^+) < 1.895$ MeV/c^2

5. There is no particle ID on the K^0_S daughters.

6. The D^+ particle ID was done in two steps.

   (a) Loose initial selection on individual tracks.

   - K/π separation for the K^-: the K hypothesis must be preferred over the π hypothesis by 0.5 units of χ^2.
   - Otherwise loose consistency.

   (b) Final selection on a per combination basis: $WSUM > 8$, where $WSUM$ is defined below.

7. For K^0_S candidates: daughters must not be included in the primary vertex.

8. For K^0_S: $0.475 \leq M(\pi^+\pi^-) \leq 0.520$ MeV

9. Use the the following types of K^0_S, defined in [4]: SSD, Track-Track, Track-Stub and Stub-Stub.

   - Stub-Stub: $\sigma_z < 7$ cm, where z is the z position of the measured K^0_S decay vertex
   - Track-Track: $\sigma_z < 9$ cm.
   - Track-Stub: $\sigma_z < 8$ cm.
   - SSD: $L/\sigma_L > 20$, where L is the decay length of the K^0_S.

The quantity WSUM is an attempt at making a single cut on the overall particle ID consistency for each combination. The idea is that if two tracks are strongly identified, it is possible to relax the cuts on the third track. This is work in progress and this analysis caught the work in the following state:

$$
\begin{aligned}
\mathrm{WSUM} &= (\mathrm{WOBS}(\pi) - \mathrm{WOBS}(K))_{K^-} \\
&\quad + (\mathrm{WOBS}(K) - \mathrm{WOBS}(\pi))_{\pi_1^+} \\
&\quad + (\mathrm{WOBS}(K) - \mathrm{WOBS}(\pi))_{\pi_2^+}. \\
&\simeq \text{Total } \chi^2 \text{ for K}/\pi \text{ separation}
\end{aligned}
$$

References

[1] A.V. Evdokimov *et al.* (SELEX Collab.), hep-ex/0406045.

[2] P L. Frabetti *et al.* (E687 Collab.), Nucl.Instrum.Meth.**A**320:519-547, 1992..

[3] J.M. Link *et al.* (FOCUS Collab.), Nucl.Instrum.Meth.**A**484:270-286, 2002.

[4] J.M. Link *et al.* (FOCUS Collab.), Nucl.Instrum.Meth. **A**484:174-193, 2002.